ELSEVIER

Contents lists available at ScienceDirect

## Journal of Biomechanics

journal homepage: www.elsevier.com/locate/jbiomech www.JBiomech.com



# Characterizing gait induced normal strains in a murine tibia cortical bone defect model

litendra Prasad\*, Brett P. Wiater, Sean E. Nork, Steven D. Bain, Ted S. Gross

Department of Orthopaedics and Sports Medicine, University of Washington, Seattle, 325 Ninth Avenue, Box 359798, Seattle, WA 98104, USA

#### ARTICLE INFO

Article history: Accepted 3 June 2010

Keywords:
Bone healing
Cortical defect model
Finite element analysis
Strain characterization
Gait analysis
Inverse dynamics

#### ABSTRACT

The critical role that mechanical stimuli serve in mediating bone repair is recognized but incompletely understood. Further, previous attempts to understand this role have utilized application of externally applied mechanical loads to study the tissue's response. In this project, we have therefore endeavored to capitalize on bone's own consistently diverse loading environment to develop a novel model that would enable assessment of the influence of physiologically engendered mechanical stimuli on cortical defect repair. We used an inverse dynamics approach with finite element analysis (FEA) to first quantify normal strain distributions generated in mouse tibia during locomotion. The strain environment of the tibia, as previously reported for other long bones, was found to arise primarily due to bending and was consistent in orientation through the stance phase of gait. Based on these data, we identified three regions within a transverse cross-section of the mid-diaphysis as uniform locations of either peak tension, peak compression, or the neutral axis of bending (i.e. minimal strain magnitude). We then used FEA to quantify the altered strain environment that would be produced by a 0.6 mm diameter cylindrical cortical bone defect at each diaphyseal site and, in an in situ study confirmed our ability to accurately place defects at the desired diaphyseal locations. The resulting model will enable the exploration of cortical bone healing within the context of physiologically engendered mechanical strain. © 2010 Elsevier Ltd. All rights reserved.

#### 1. Introduction

Bone's mechanical environment has an important role in regulating the complex process of bone healing (Claes and Heigele, 1999; Isaksson et al., 2006). Not surprisingly, cellular and tissue responses associated with bone healing are sensitive to a variety of mechanical stimuli, which include principal strain, hydrostatic stress, deviatoric strain, shear strain, and fluid velocity (Claes and Heigele, 1999; Isaksson et al., 2009; Lacroix and Prendergast, 2002). However, the predominance of studies in this area has examined bone healing in the context of externally applied non-physiological mechanical stimuli, where non-physiological loading induced stimuli refer to those not engendered by normal animal activities, but rather by an external loading device.

In considering potential models to explore how mechanical stimuli engendered by physiologic loading interact with biological healing of bone defects, the mouse presents obvious potential for exploration of specific signaling pathways. As might be expected, a number of fracture healing models originally developed in larger animals (Connolly et al., 2003; Isaksson et al., 2009; Wang et al., 2007)

have been recently implemented in mice. However, just as the small size of the murine skeleton challenged development of *in vivo* bone healing models, quantification of physiologically induced bone strains in mice (De Souza et al., 2005) has also proven challenging compared with larger animals (Blob and Biewener, 1999; Demes et al., 2001; Gross et al., 1992; Rubin and Lanyon, 1982, 1984). Regardless of the stature of the animal, however, long bones are generally loaded in bending about a consistent plane during the stance phase of gait (Biewener and Dial, 1995; Main and Biewener, 2004; Moreno et al., 2008; Rubin and Lanyon, 1982, 1984). Consequently, cortical regions of long bone diaphyses are consistently exposed to minimal normal strain (i.e. the neutral axis), tension or compression (Demes et al., 2001, 1998; Gross et al., 1992; Lieberman et al., 2004; Mason et al., 1995).

In this study, our objective was to develop a mouse model that will enable exploration of how mechanical stimuli mediate bone healing in the context of physiologically induced bone deformation. To achieve this goal, we first used an inverse dynamics and finite element analysis approach to quantify the normal strains induced in the mouse tibia during the stance phase of walking. We then investigated the effect of placing uni-cortical defects through the diaphysis in three regions within the same diaphyseal cross-section consistently exposed to distinct mechanical stimuli during locomotion: (1) anterior cortex (tension), (2) posterior cortex (compression), and (3) medial cortex (neutral axis) on

<sup>\*</sup> Corresponding author. Tel.: +1 206 897 5609; fax: +1 206 897 5611.

E-mail address: prasadj@u.washington.edu (J. Prasad).

normal strains induced by locomotion. We then hypothesized that it would be possible to locate cortical bone defects such that physiological loading alone would expose healing bone to distinct types of mechanical stimuli.

#### 2. Methods

#### 2.1. Inverse dynamics

Joint angles and hip crest height as a function of normalized time (during stance phase) were derived from two previous studies (Akay et al., 2006; Leblond et al., 2003). To model adult (16 week old) C57BL6/J female mice that have been used throughout this study, the following segment lengths were used: hip (ilium) 5.00 mm, femur 14.95 mm, tibia 16.73 mm, foot (carpals and metacarpals) 7.23 mm, and toe (phalanges) 6.60 mm (Leblond et al., 2003; Lepicard et al., 2006). Segments were assumed to be one-dimensional rigid links (bars) whose relative motion (kinematics) was determined by the joint angles and hip crest height. Murine hindlimb kinematics were then determined for 11 equidistant time points—from initiation of the stance (phase 0.0) through the completion of the stance (phase 1.0; Fig. 1a).

For this study, we considered a gait velocity of 0.3 m/s, representing the maximal gait speed for caged mice (Neumann et al., 2009; Serradj and Jamon, 2009). Data for the horizontal (anteroposterior) and vertical ground reaction forces generated during walking (corresponding to a mouse of 24 g weight) were directly adapted from the work of Zumwalt et al. (2006). The horizontal ground reaction force in the medial–lateral direction was neglected given the unavailability of 3-D motion data, and our model therefore assumed that hind-limb motion was planar.

Using the kinematics and ground reaction force data, ankle moments were calculated as a function of normalized time (i.e. stance phase). This moment, at any point in time, was balanced by the calf muscle moment. The mean ( $\pm$ S.E.) moment arm for the calf muscle at the ankle was experimentally determined by measuring the horizontal distance between Achilles tendon attachment to calcaneus and the center of proximal talus in separate C57 (n=4) mice to be  $1.27 \pm 0.15$  mm, which enabled determination of calf muscle force as a function of normalized time. By transferring the ground reaction forces and the calf muscle force to the distal end of tibia, resolved forces (longitudinal (or normal) and shear) acting on tibia were determined (Fig. 1b).

#### 2.2. Characterization and validation of gait induced normal strains

We first carried out  $ex\ vivo$  strain gage experiments on intact hindlimbs (tibia and fibula) taken from a 16 week female C57 mice (n=3). Single element strain gages were attached to the anterior/lateral and medial/posterior cortices of each specimen. Each specimen was then potted at the proximal end with the distal tibia subjected to a range of normal  $(0.5-2\ N)$  in steps of  $0.5\ N$ ) and shear static loads  $(0.05\ N-0.3\ N)$  in steps of  $0.05\ N$ ). This range of end loads spanned the magnitude of gait induced resolved forces for locomotion at  $0.3\ m/s$ . For each specimen, the relationship between applied end load and induced normal strain was linear within the range of assessed loads.

The specimens were then scanned with 21 µm voxel size (SCANCO VivaCT 40). Using an in-house computer program developed using Microsoft Visual Basic 2005, the  $\mu\text{CT-scan}$  images were transformed to a voxel-based FE model (made of 8-noded hexahedral elements). The meshing algorithms in the program had been thoroughly debugged via comparison with commercial FE softwares (ABAQUS, ANSYS, and Patran/Nastran). The material properties (Young's modulus: 20 GPa and Poisson's ratio: 0.3) were derived from the literature for adult female C57 mice (Akhter et al., 2004; Brodt et al., 1999). For each specimen, FE analysis was carried out for each of the 11 stance phase time points using shareware FEM software CalculiX (Dhondt and Wittig, 2008). Normal strains were resolved for the whole bone, with mid-diaphyseal normal strains numerically quantified and compared to the measured strain gage data (strain gage attachment sites identified via CT imaging). These data were assessed qualitatively in the context of hindlimb anatomy (to minimize soft tissue damage during surgery) to identify a transverse diaphyseal region in which cortical defect sites could be placed in regions of cortex exposed to distinct normal strains throughout the stance phase of gait (1.5 mm proximal from the tibia-fibula junction).

#### 2.3. Normal strain alterations due to cortical bone defects

Following verification of our ability to quantify tibia normal strain distributions in intact tibias, we used FEA to parametrically explore the effects of cortical bone defects on normal strain magnitudes around the defect. A 0.6 mm-diameter cylindrical bone defect through one cortical surface was created *in silica* at diaphyseal locations continually exposed to 3 distinct types of mechanical stimuli: (1) anterior cortex (the site of peak tension), (2) medial cortex (spanning the medial neutral axis), and (3) posterior cortex (the site of peak compression). The defects were 1.5 mm proximal from the tibiofibular junction in each of the three tibia FE models. The chosen defect size (0.6 mm diameter) was within the range of common drill-hole sizes (0.5–1.0 mm) found in the literature and reflected a balance of surgical accessibility and size of the mouse tibia cortex (Campbell et al., 2003; Kim et al., 2007).

For boundary conditions corresponding with peak induced strain during the stance phase, two measures were assessed to define strain alterations arising from the cortical defect at the time of peak strain. First, the strain concentration factor was determined as the ratio of maximal induced normal strain around the defect to the maximal induced normal strain for that cortical region in an intact tibia, where the maximal strain was defined as the greatest centroidal strain (i.e. the greatest average elemental strain) and was found to roughly correspond to the 97th percentile. Second, peak strain energy density was determined within a 0.1 mm ring of cortex surrounding each defect site. We then considered alterations in total strain energy across the entire stance phase by integrating strain energy density within the 0.1 mm ring surrounding each defect site across each of the 11 boundary condition solutions defined for the stance phase gait at 0.3 m/s and these data were compared to those derived for the same cortical sites in an intact tibia.

Last, to confirm surgical feasibility of our approach, we drilled  $0.6\,\mathrm{mm}$  diameter holes at each diaphyseal locations ( $n{=}4\,\mathrm{mice}$  per location in a survival surgery) using a micro-drill (Ideal Micro-Drill, model MD-1200, Braintree Scientific). The hole placement was targeted 1.5 mm proximal to tibiofibular junction. To quantify the actual hole location with respect to the target location,

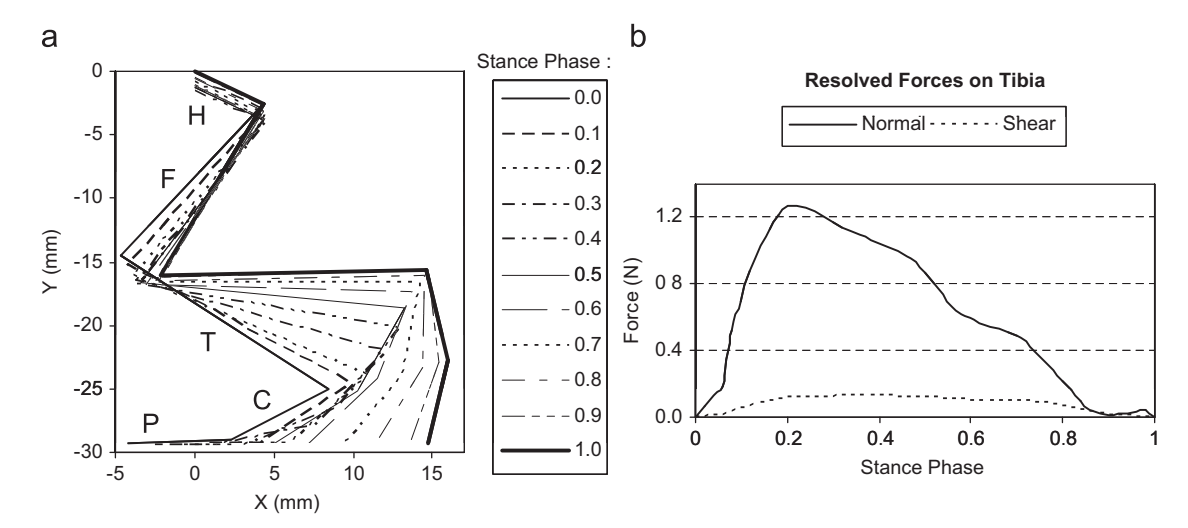


**Fig. 1.** Kinematics and kinetics of murine hindlimb during stance phase. Segment lengths for the hip (H), femur (F), tibia (T), foot (carpal and metacarpal; C), and phalange (P) are noted (a). Rigid body motion of the hindlimb was determined for 10 equal intervals through the stance phase (0.0=stance initiation, 1.0=stance completion). Rigid-body kinematics of the hindlimb and the ground reaction forces from the literature were used to resolve the total force acting on the distal tibia through the stance phase (b). The total force was resolved into axial force acting along the tibia long axis and shear force in anterio-posterior axis.

### Download English Version:

# https://daneshyari.com/en/article/872595

Download Persian Version:

https://daneshyari.com/article/872595

Daneshyari.com